International Journal of Fluid Machinery and Systems
Vol. 4, No. 1, January-March 2011

DOI: 10.5293/IJFMS.2011.4.1.150
ISSN (Online): 1882-9554

Original Paper (Invited)

Efficiency of Marine Hydropower Farms Consisting of Multiple Vertical Axis Cross-Flow Turbines

Andrei-Mugur Georgescu[1], Sanda-Carmen Georgescu[2], Costin Ioan Cosoiu[1] and Nicolae Alboiu[1]

[1]Hydraulics and Environmental Protection Dept, Technical University of Civil Engineering Bucharest
124 Bd. Lacul Tei Sector 2, Bucharest, RO-020396, Romania, andrei_georgescu2003@yahoo.com, costin@hidraulica.utcb.ro, nalboiu@hidraulica.utcb.ro
[2]Hydraulics and Hydraulic Machinery Department, University "Politehnica" of Bucharest
313 Spl. Independentei Sector 6, Bucharest, RO-060042, Romania, carmen.georgescu@upb.ro

Abstract

This study focuses on the Achard turbine, a vertical axis, cross-flow, marine current turbine module. Similar modules can be superposed to form towers. A marine or river hydropower farm consists of a cluster of barges, each gathering several parallel rows of towers, running in stabilized current. Two-dimensional numerical modelling is performed in a horizontal cross-section of all towers, using FLUENT and COMSOL Multiphysics. Numerical models validation with experimental results is performed through the velocity distribution, depicted by Acoustic Doppler Velocimetry, in the wake of the middle turbine within a farm model. As long as the numerical flow in the wake fits the experiments, the numerical results for the power coefficient (turbine efficiency) are trustworthy. The overall farm efficiency, with respect to the spatial arrangement of the towers, was depicted by 2D modelling of the unsteady flow inside the farm, using COMSOL Multiphysics. Rows of overlapping parallel towers ensure the increase of global efficiency of the farm.

Keywords: Achard turbine, cross-flow current turbine, hydropower farm, farm efficiency, force coefficient, power coefficient.

1. Introduction

The Achard turbine is a new concept of vertical axis, cross-flow, marine current turbine module [1], developed within the French HARVEST Project (abbreviated from Hydroliennes à Axe de Rotation VErtical STabilisé), launched since 2001 in Grenoble, at LEGI (Geophysical and Industrial Fluid Flows Laboratory), with the support of the R&D Division of the Électricité de France Group. The main advantages of the Achard turbines are their modularity, and their ability to operate irrespective of the water flow direction. Thus, similar modules (that allow series industrial production) can be superposed on the same vertical axis, to form towers, with lengths adapted to marine or river current depths, at different locations. A marine or river power farm consists of a cluster of barges, each barge gathering several towers. Within a barge, several parallel rows of towers can be put in non-overlapped, or in overlapped staggered arrangements. For the former case, the turbines of the downstream row are not placed in the wake of the upstream turbines. The optimum spatial arrangement of the towers in the farm corresponds to the best overall efficiency. We found that rows of overlapping towers ensure the increase of global efficiency of the farm.

To be able to assess this optimal arrangement in the simplest way possible, i.e. by two-dimensional numerical modelling, we had to make sure that our numerical model was accurate with respect to experimental results. Hence, a simple 1:5 scale model of a hydropower farm equipped with three Achard turbines was built and tested in a variable slope water channel at the Hydraulics Laboratory of the Technical University of Civil Engineering Bucharest (UTCB).

2. Achard Turbine Module and Farm Description

The Achard turbine consists of a runner with three vertical delta blades (Fig. 1), sustained by radial supports at mid-height of the turbine. The blades are shaped with NACA 4518 airfoils, while the radial supports are shaped with straight NACA 0018 airfoils. The turbine main dimensions are: the runner diameter D = 1 m and the runner height H = 1 m. Within the 3D Cartesian coordinate system, along each delta blade, the airfoil mean camber line length varies from 0.18 m at mid-height of the turbine (where z = 0), to 0.12 m at the extremities (where $z = \pm H/2$). A simple hydropower farm model, equipped with three Achard turbine modules (Fig. 2), has been built at 1:5 scale [2], to be tested in the water channel at the Hydraulics Laboratory of UTCB. Due to the channel depth limitations, the turbines cannot be superposed to form towers.

Accepted for publication December 23, 2010: Paper number O10060S
Corresponding author: Andrei-Mugur Georgescu, Associate Professor, andrei_georgescu2003@yahoo.com
This manuscript was presented at the 25th IAHR Symposium on Hydraulic Machinery and Systems, September 20-24, 2010, Politehnica University of Timisoara, Romania.

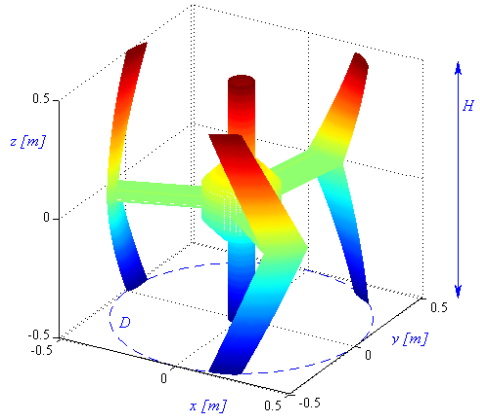

Fig. 1 Achard turbine geometry generated analytically in MATLAB

Fig. 2 Farm model at 1:5 scale, with 3 Achard turbines, here aligned on a row across the channel longitudinal axis (viewed from upstream)

The Achard turbines run in stabilized current, so the flow can be assumed to be almost unchanged in horizontal planes along the *z*-axis. This assumption allows performing 2D numerical modelling, for different arrangements of the towers within the farm. Being a 2D approach, the results apply to other vertical axis cross-flow turbine modules, e.g. Darrieus, or Gorlov modules.

Vertical axis cross-flow turbines present much more complex flow patterns between the blades than classical axial, free stream turbines. In the former case, for a given horizontal position along the blades and a given velocity U_∞ of the current (e.g. pointing in the *Ox*-direction), the angle of attack α and the relative velocity w change constantly during a complete rotation, defined by the azimuthal angle θ, from 0º to 360º (Fig. 3). As a consequence, the lift and drag forces acting on the blades change also during a complete rotation. Those forces can be decomposed with respect to the rotation circle, as normal force F_n and tangential force F_t (Fig. 4). The resulting total tangential force is the one responsible for turbine rotation, provided it points in the same direction as the transport velocity ωR.

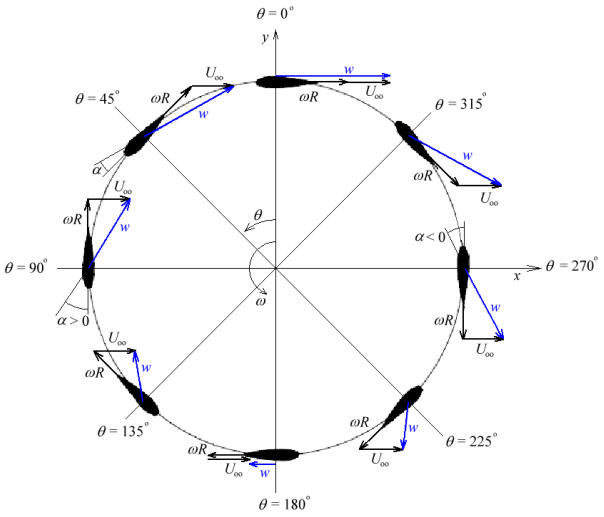

Fig. 3 Water relative velocity w and angle of attack α with respect to the blade position θ

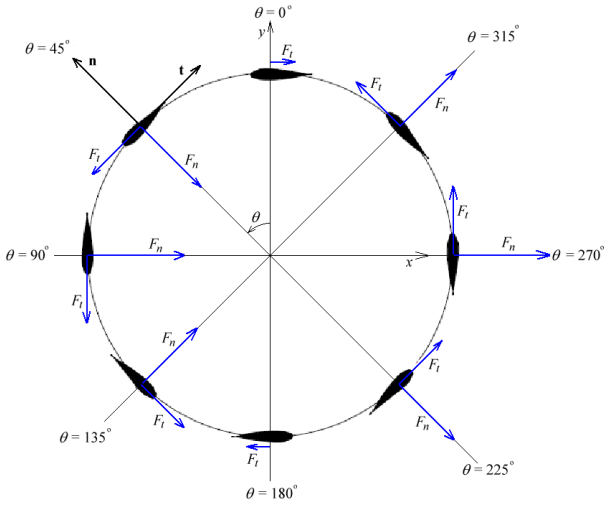

Fig. 4 Normal force F_n and tangential force F_t with respect to the blade position θ

There are two critical zones: an upper zone around θ = 0º, and a lower zone around θ = 180º, where the tangential force is negative and opposes the rotation. In order to increase the efficiency of such turbines, the influence of these zones should be reduced as much as possible. There is tough a difference between the two critical zones. If the upstream water velocity U_∞ increases, then around θ = 0º, the relative velocity w will increase also, and consequently, the negative tangential force F_t will increase, while around θ = 180º, the relative velocity will decrease, and consequently, the negative tangential force will decrease also. In other words, if one could increase the velocity of the current around θ = 180º and decrease it around θ = 0º, then the negative tangential force would be reduced and the turbine efficiency would be increased. Of course, this is just a theoretical case. In fact, in Figs 3 and 4, it has been assumed that the blade is subjected to a constant upstream velocity distribution, independent of its position. This is a good assumption for any position of the blade in the first half rotation, for θ = 0º÷180º. But for θ = 180º÷360º, due to dynamic stall, the blades are subjected to a different velocity profile. The local water velocity along a line on the *Oy*-direction that crosses the turbine at its axis is denoted by *U*. In accordance with the *U* velocity profile along the mentioned line [3], for different time moments during the second half rotation of the turbine, the resulting forces on the blade during the second half

rotation are different with respect to the theoretical case presented above.

Within the present paper, the numerical tests concerning the efficiency of the farm were carried out by taking an upstream flow velocity U_∞ = 1 m/s, and an angular velocity of the turbine $\omega = \pi$ rad/s (meaning a rotational speed of 30 rpm), during 12 seconds, which represents 6 full rotations of the turbine. The time step was of 0.05 seconds. No data was recorded for the first 5 turns of the turbine, and only the 6th complete turn was used to yield results.

The blade positioned at $\theta = 0^\circ$ at the start of the rotation will be termed as the first blade. The blade that starts moving at $\theta = 120^\circ$ will be termed as the second blade, while the one that starts at $\theta = 240^\circ$ will be termed as the third blade. For an isolated Achard turbine, the polar representation of the tangential force acting on the first blade, for a complete rotation, shows that the tangential force is negative only in the upper critical zone of the turbine, from $\theta \cong -55^\circ$ (or $\theta \cong 305^\circ$) to $\theta \cong 40^\circ$. If all three blades of the isolated turbine are considered, the polar curves corresponding to the last two blades will resemble to the polar curve of the first blade, only shifted with almost 120º and 240º respectively.

The total tangential force, obtained as the sum of the tangential forces acting on the three blades at each time step, presents 3 positive minima, at $\theta = \{36^\circ; 162^\circ; 279^\circ\}$, and 3 maxima, placed at $\theta = \{108^\circ; 225^\circ; 342^\circ\}$. The variations of the tangential force on the 3 blades, as well as, the variation of the total tangential force are presented in Fig. 5, with respect to the time moment of the full rotation, which takes 2 seconds. As the total tangential force for an isolated turbine results only in positive values, one can assume that by increasing its minimal values, the turbine efficiency will increase.

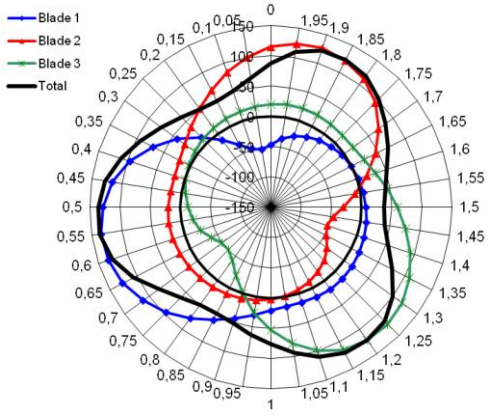

Fig. 5 Polar representation of F_t on the 3 blades, and total tangential force, upon the time moment of the full rotation

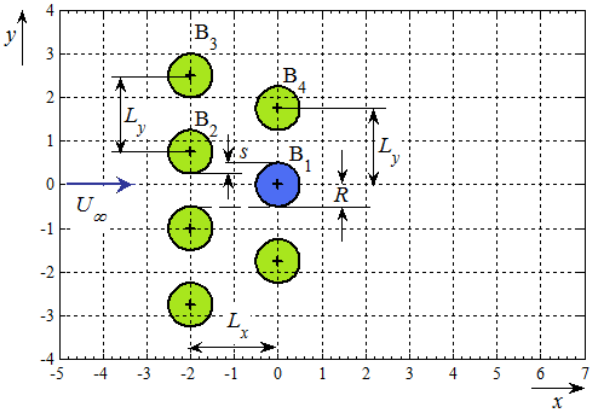

Fig. 6 Farm configuration with 7 staggered turbines on 2 rows; overlapping between upstream & nearest downstream turbines

All values of the total tangential force can be increased, by arranging the towers (turbines) within the farm in staggered parallel rows: thus, the turbines on the downstream row will work in a somehow confined space, with respect to the ones on the upstream row, and the farm global efficiency will increase. At first sight, it seems that to avoid inter-influence between rows, turbines on the downstream row must not be placed in the wake of the upstream turbines [4], but there are better solutions [3]. In fact, in order to increase turbine efficiency for a given transport velocity ωR and a given upstream water velocity U_∞, one should decrease the water velocity in the upper critical zone of the turbine. This will be achieved further, by arranging the towers (turbines) within the farm in a somehow unusual staggered rows configuration, namely in overlapped parallel rows, thus yielding better efficiencies for the towers in the second row facing the flow.

Two similitude numbers characterise the Achard turbine: the tip speed ratio $\lambda = \omega R / U_\infty$ and the solidity $\sigma = cB/R$, where the turbine radius is R = 0.5 m and the number of blades is B = 3. The 2D computational domain is a cross-section of all towers at a certain z-level, namely $z = H/4$ in this paper, where the airfoil chord length is $c \cong 0.15$ m. Thus, the value of the tip speed ratio λ equals $\pi/2$, being different than the usual value, $\lambda = 2$, prescribed for the Achard turbine [5]. The solidity value is $\sigma = 0.9$.

As the turbine efficiency depends both on the upstream water velocity U_∞ and on the spatial arrangement of the towers (turbines) within the farm, one must define the gap between two successive axes. Within the xOy plane, the distance between two adjacent rows of turbines is denoted by L_x and the distance between axes of 2 adjacent turbines on each row is denoted by L_y (e.g. $L_y = 2D$ in Fig. 2). The overlapping between the upstream turbine and the nearest downstream turbine is denoted by s, as in the farm configuration presented in Fig. 6. For $s = 0$, the rows are in a non-overlapped staggered configuration.

There are some key positions of the towers (turbines), denoted from B_1 to B_4 in Fig. 6, which are relevant to determine the farm global efficiency: the turbine placed in B_1 is fully influenced by the upstream row, the one placed in B_2 is influenced by the adjacent turbines and downstream ones, while the turbines placed in B_3 and B_4 are subjected to end-of-row effects.

3. Experimental Setup

The experimental tests were performed in the variable slope, open channel of the Hydraulics Laboratory of UTCB (Fig. 7.). That water channel has the following dimensions: 1.2 m wide, 0.8 m deep, and 28 m long. The farm model has been placed at mid length of the channel. The turbine models were built at 1:5 geometric scale, resulting with D = 0.2 m diameter and H = 0.2 m height. In order to achieve the desired experimental flow conditions, the channel slope was set at 1‰ and a water depth of 0.36 m was ensured. The Achard turbines were disposed within the C1, C2 and C3 farm configurations as shown in Fig. 8, with $2D$

distance between 2 adjacent turbine axis, namely: C1 with turbines aligned on a single row, across the flow direction (as in Fig. 2); C2 with isosceles triangular arrangement pointing downstream (with two front turbines); C3 with isosceles triangular arrangement pointing upstream (with a single front turbine). A mean water velocity of 0.53 m/s was ensured in the channel for the C1 farm model. Due to the failure of one of the supply pumps, only a 0.51 m/s mean water velocity was ensured in the channel for the C2 and C3 farm models.

Fig. 7 Experimental set-up: Variable slope open channel, with turbines in an isosceles triangular arrangement pointing upstream, viewed from downstream (left); Acoustic Doppler Velocimeter sensor placed in the wake of the farm model (right)

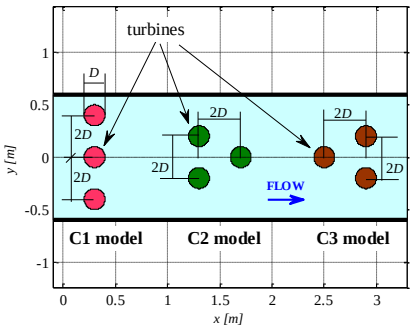

Fig. 8 Farm configurations: C1/ Single row; C2/ Triangular, 2 front turbines; C3/ Triangular, a single front turbine

Using the similitude conditions derived for such vertical axis turbines by Georgescu et al. [5], the prescribed value of the tip speed ratio λ for the Achard turbine equals 2. Accordingly, the computed value of the rotational speed of the turbines in the C1 farm model (which would assure the same tip speed ratio as the real module) equals 101.2 rpm, meaning an angular velocity ω = 10.6 rad/s, while for the C2 and C3 farm models, the rotational speed is of 97.4 rpm, meaning ω = 10.2 rad/s. The turbine models are driven by electrical motors provided with variable speed, to insure the computed rotational speed.

Experiments were performed in two steps: ① the first step focused on the calibration of the channel, by measurement of the mean water velocity in the channel (with an ultrasonic flowmeter), and measurement of the velocity distribution with channel depth, at mid-width of the channel (with the Acoustic Doppler Velocimeter). From the vertical velocity profile, we retained the value of the local velocity at the submerged level placed at $z = H/4$ relative to the median turbine plane: that local velocity was denoted in this paper as upstream velocity of the water, U_∞. All subsequent water velocities measured in the channel, will be divided in this paper by the upstream velocity U_∞. The same velocity U_∞ was introduced in the validation numerical models as input boundary condition; ② the second step focused on effective measurements of the average over a full turbine rotation of the velocity distribution, downstream of the turbines ensemble.

The water velocity distribution was measured using a 3D Acoustic Doppler Velocimeter (ADV), which is a versatile, high-precision instrument that measures all three components of the velocity, at a given sampling point, defined by a tiny water volume. The measurements are insensitive to water quality. The ADV uses acoustic sensing techniques to measure flow in a remote sampling volume (6 mm long and approximately 6 mm in diameter), which is located away from the sensor to provide undisturbed measurements. Doppler velocity is derived from signals scattered by small particles. Data are available at an output rate of 25 Hz. The considered sampling points were aligned on a so-called "reference line," namely a horizontal line in *Oy*-direction, which was placed two and a half turbine diameters ($2.5D$) downstream of the last turbine reached by the flow, and was immersed at a level $z = H/4$ relative to the median turbine plane. The reference line, with a minimum length of 0.64 m, was centred to the channel longitudinal axis. The sampling density was set at 1 measurement per centimetre. The average over a full turbine rotation of the velocity distribution could be plotted in dimensionless values (divided by the upstream velocity), along the reference line.

4. Validation

Two different numerical approaches were performed, one in FLUENT using the exact numerical replica of the experimental setup, and the other in COMSOL Multiphysics using a simplified numerical model.

4.1 Numerical Setup in FLUENT

In FLUENT, the transient flow simulations were performed as in Georgescu et al [6], for a two-dimensional fluid domain, included in the so-called "reference plane," a horizontal plane that intersects the turbines at a level $z = H/4 = 0.25D$ relative to the median turbine plane. The computational domain in the *xOy* plane was built at the same scale as the experimental model, its width being equal to that of the channel where the experimental tests were conducted. The computational domain extent was set horizontally for $x \in [-4D; 7D]$, and vertically for $y \in [-3D; 3D]$, resulting in a 2.2 m × 1.2 m rectangle. To capture the effects of rotating blades, a sliding mesh model (SMM) was used. Thus, circular areas centred on the axes of rotation of the 3 turbines, with a diameter of 0.24 m, were considered to rotate with angular velocity ω. The computing grid was a mixed one, made from quad type cells, smaller near the solid surfaces and larger in the free stream zone. The total number of cells was equal to 216497 for the C1 farm model, with a minimum characteristic size of 0.1 mm in the boundary layer areas, adjacent to solid surfaces. The computational mesh attached to each of the 3 farm configurations, denoted C1, C2 and C3, are presented in Fig. 9.

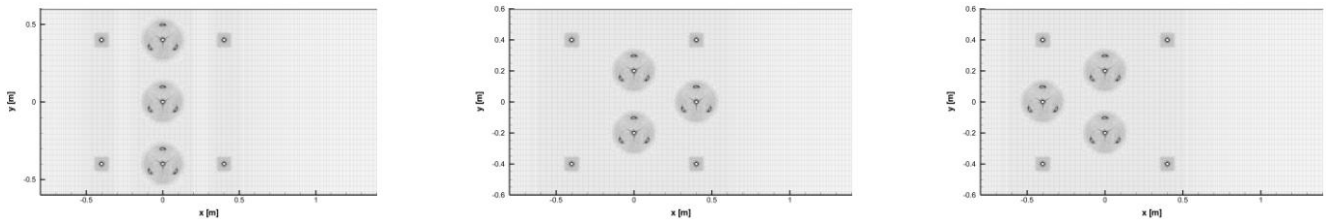

Fig. 9 Computational mesh for the farm models in FLUENT: C1 (left frame), C2 (middle frame) and C3 (right frame)

At the inlet section (left hand side of the domain), a uniform velocity distribution was considered, with a magnitude U_∞ = 0.57 m/s for C1 tests, and U_∞ = 0.54 m/s for C2 & C3 tests. In the outlet section (right hand side of the domain), the pressure was designated to be equal to zero, gage scale. On all solid surfaces, a no-slip condition was considered. Rotating fluid domains moved with an angular velocity ω, where ω = 10.6 rad/s for C1 tests, and ω = 10.2 rad/s for C2 & C3 tests. Around the turbine, the flow regime is turbulent, characterized by parameters that fluctuate strongly in time. Therefore, to capture as accurately as possible the velocity and pressure fields in the considered computational domain, a $k-\varpi$ Shear Stress Transport (SST) turbulence model was adopted, where k is the turbulent kinetic energy, and ϖ is the specific turbulent dissipation rate. The chosen solver was a double precision, pressure-based coupled one. To obtain a good discretisation of the momentum, continuity and turbulence model specific equations, second-order discretisation schemes were used. The time of the simulation corresponds to 10 complete rotations of the turbines. Only the last full rotation was considered in the sequel for the velocity distribution.

To accurately reproduce the near-wall ϖ variation (in the viscous sublayer), Wilcox [7, page 277] imposes to keep very low the dimensionless sublayer-scaled distance y^+, namely $y^+ < 2.5$, while Blazek [8, page 247] recommends to refine the grid such that $y^+ < 3$. In our computations, the y^+ parameter, computed for all farm configurations at the wall boundaries of the active parts (shaft and blades) of the turbines, was lower than 1 for 75.7% up to 80% of the total cells, between 2.5 and 3 for only 0.53% down to 0.35% of cells, and between 1 and 2.5 for the remaining cells. Refining the grid (using y^+ adaption in FLUENT), i.e. to obtain $y^+ \leq 1$ for all cells, will ensure a grid independent solution, but a finer grid will increase excessively the computational time, and that is beyond the purpose of the study: the goal is to obtain a numerical tool to get results as quick as possible, within an acceptable accuracy. The numerical results will help only to select best farm configurations, which will be further exhaustively investigated experimentally. As we will show further in this section, the results fit well enough downstream of the middle turbine (the area of interest); obviously, one cannot expect to obtain a perfect match, since the numerical model is a two-dimensional one, while experiments were conducted in the 3D space.

4.2 Numerical Setup in COMSOL Multiphysics

In COMSOL Multiphysics, the transient flow simulations were performed as in Georgescu et al [6], for a 2D fluid domain, included in the above defined "reference plane," at $z = 0.25D$. The numerical model of the turbine was built at 1:1 geometrical scale, as the real Achard turbine (with D = 1 m), so the open channel was set to be 5 times bigger (i.e. 6 m wide) than the channel used in the experimental setup. The computational domain was set to 12 turbine diameters long and 6 turbine diameters wide (resulting in a 12 m × 6 m rectangle), defined by $x \in [-5D; 7D]$ and $y \in [-3D; 3D]$. The computational mesh for the C1 farm model consisted of 5016 triangular elements, 426 boundary elements and 154 vertex elements, yielding 44543 degrees of freedom. The computational mesh attached to each of the 3 farm configurations (C1, C2 and C3) are presented in Fig. 10.

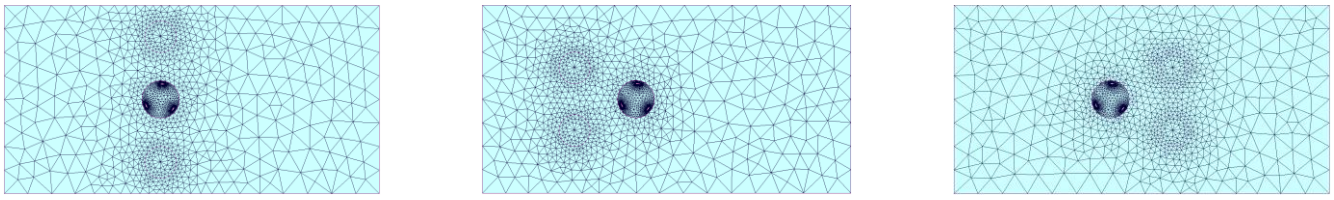

Fig. 10 Computational mesh for the farm models in COMSOL: C1 (left frame), C2 (middle frame) and C3 (right frame)

The simulations were performed under a time dependent flow regime with a time step of 0.05 seconds. The flow was considered turbulent, with a $k-\varepsilon$ turbulence model, where ε is the dissipation of turbulence per unit mass. The boundary conditions used were: water inlet with the velocity U_∞ = 0.57 m/s for C1 tests, and U_∞ = 0.54 m/s for C2 & C3 tests (on the left hand side of the domain); water outlet with no viscous stress (on the right hand side of the domain); rough wall computed with the logarithmic wall function with an offset of $h/2$ on the top and bottom of the domain, as well as on the blades of the turbine; all other boundaries were set to neutral.

In order to gain computational time, we used only one rotating turbine, the two other turbines (fictitious turbines) being modelled based on the action-reaction principle from a single rotating turbine model, as we will show further in Section 4. Due to the change of the geometrical scale, the angular velocity of the rotating turbine was set to ω = 2.12 rad/s for the C1 farm model, and ω = 2.04 rad/s for the C2 & C3 farm models. The time of the simulation corresponds to 8 complete rotations of the turbine. Only the last full rotation was considered in the sequel for the velocity distribution.

To determine the optimal grid, a preliminary grid dependency test was carried out in Georgescu et al [6]. For all farm models,

the meshes from Fig. 10 are the normal ones (the 5th among 9 predefined settings, ranging from extremely coarse to extremely fine). As we will show further, in Section 3.3, the results attached to the normal mesh are quite superposed on fine mesh's results, and fit well experimental results. The normal mesh was selected, since it ensures a shorter computational time.

4.3 Comparison between Experimental and Numerical Results

The numerical results and measured experimental data concerning the dimensionless velocity distribution, as ratio between the average of the velocity over a full turbine rotation, and the upstream velocity U_∞, along the "reference line" placed at 2.5D downstream of the turbines, are presented in Figs. 11÷13, for the studied farm configurations (C1, C2 and C3). For the C3 model (Fig. 13), besides the COMSOL results for the normal mesh (red line), we added the results for a coarse mesh, and for a fine mesh.

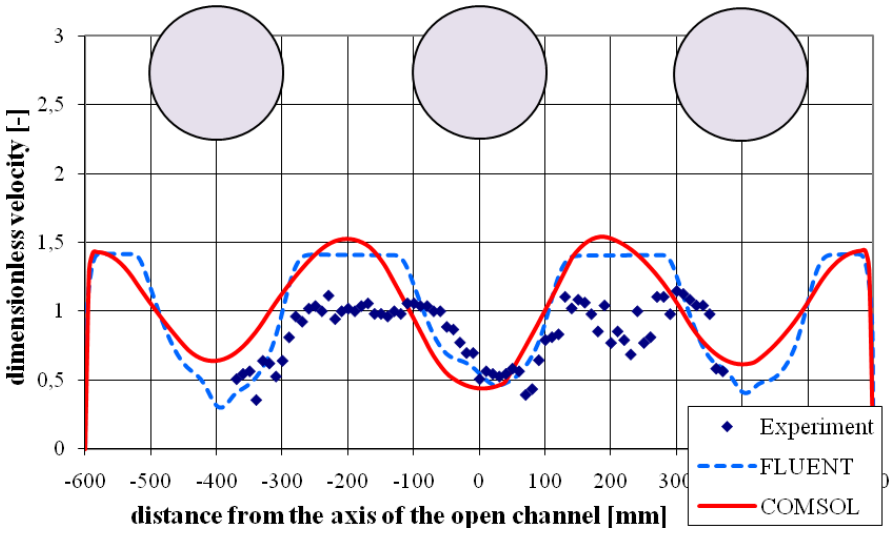

Fig. 11 Comparison between numerical & experimental dimensionless velocity distribution on the reference line, for the C1 farm

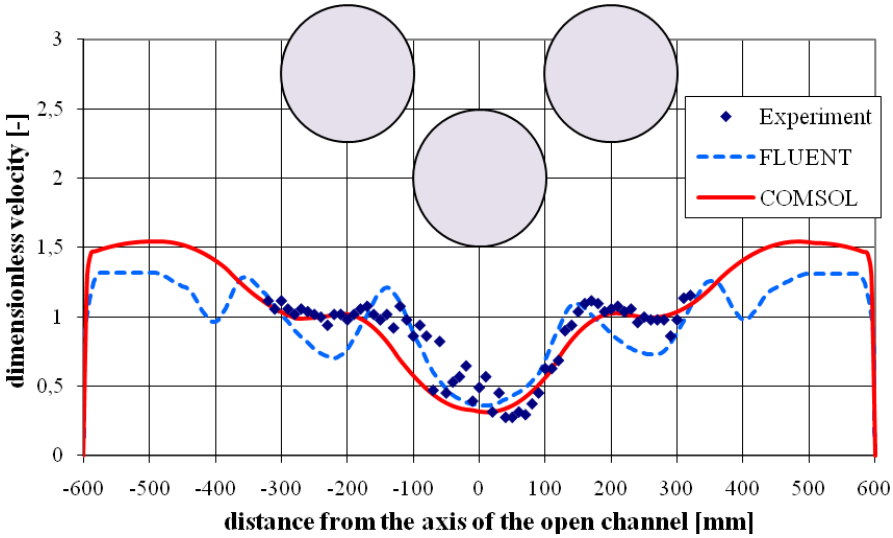

Fig. 12 Comparison between numerical & experimental dimensionless velocity distribution on the reference line, for the C2 farm

From Figs. 11÷13 we can see that the trends of the numerical curves and experimental points are somehow similar. A better fit seems to occur for both triangular farm models. For the C1 model, the numerical values are closer to one another, while the experimental ones (especially between the turbines) are smaller, as reported by Georgescu et al. [9]. This discrepancy is probably due to the fact that for the numerical simulations we used a two-dimensional model. For the experimental model, water can by-pass the turbines, by flowing above or below, not only sideways as in the simulations.

Moreover, we can see from all the 3 graphs (Figs. 11÷13), that the influence of the turbines downstream is larger than the actual diameter of the turbine. In fact, it is the largest in COMSOL (which is the less accurate numerical model), and the smallest in the experimental case. In either of the triangular arrangements, this increased influence would be combined with influence of the adjacent turbine, and yield between the turbines, a different result (basically smaller velocities) in COMSOL. In a line arrangement, the increased influence of the turbines would add up for the numerical 2D models, to yield a stronger blockage effect of the cross section, and hence, greater velocity values between the turbines.

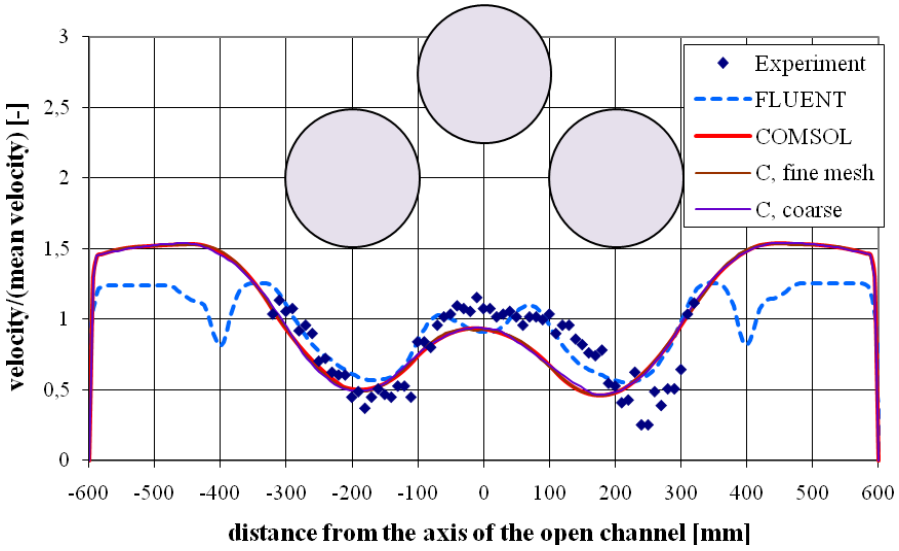

Fig. 13 Comparison between numerical & experimental dimensionless velocity distribution on the reference line, for the C3 farm. The wide red line corresponds to COMSOL Multiphysics results obtained with the normal mesh, the brown line to fine mesh's results, and the magenta line to coarse mesh's results

4.4 Validation Conclusions

The differences between the performed test should be put in terms of time and energy consumption, in order to establish if they are worth performing in the future, or not. One set of experimental tests took about 8 hours to perform. During this time, at a flow rate of 0.22 m^3/s, about 155 kWh were consumed. At this, we have to add the time and costs necessary to build the experimental farm model itself, the calibration of the open channel etc. The FLUENT farm model needed 3 days to compute each configuration on a 4-processors workstation with 8 GB RAM. The COMSOL farm model, with a normal mesh, needed about 8 hours to compute each configuration on a mobile workstation with 2 GB RAM.

If we consider the amount of resources needed for each of the tests, the differences between the curves and points presented in Figs. 11÷13 tend to shrink. Of course, the simplified COMSOL model is the less accurate, but it can be used relatively quickly for the characterisation of different more complicated arrangements of the turbines. The more accurate FLUENT model can be used in the sequel, for the characterisation of a final arrangement. Of course, this final arrangement should also be modelled experimentally, in order validate the numerical results.

5. Numerical Approach Efficiency

The two-dimensional numerical modelling of the unsteady flow inside a hydropower farm consisting of several Achard turbines (towers), placed in different spatial arrangements, has been performed by using the code COMSOL Multiphysics. In order to diminish the computational effort, the geometry has been simplified, by neglecting the vertical shaft of the turbine, so only the three airfoils, corresponding to the delta blades, will appear in a turbine (tower) cross-section.

The computational mesh for an isolated turbine (tower), rotating counter clockwise, is presented in Fig. 14. The investigated domain extension was 12 turbine diameters long (from $x = -5$ m to $x = 7$ m along the flow direction), and 8 turbine diameters wide (from $y = -4$ m to $y = 4$ m across the flow). The model of the turbine was placed with its axis at $\{x = 0; y = 0\}$.

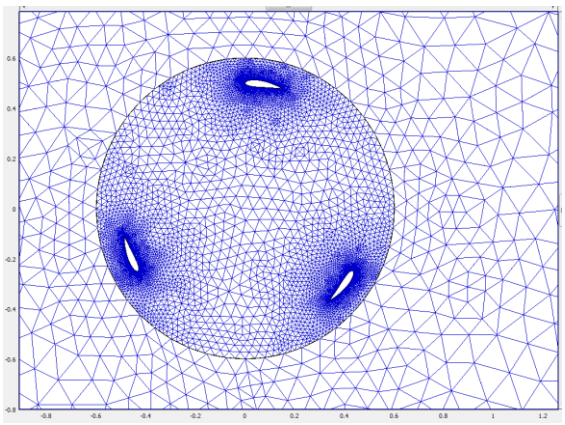

Fig. 14 Computational mesh for an isolated turbine (zoom)

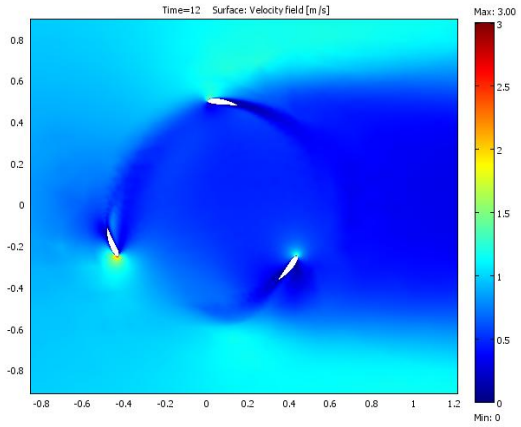

Fig. 15 Velocity field for an isolated turbine (zoom)

The unstructured mesh with triangular elements, boundary elements, vertex elements and about 39500 degrees of freedom, consists of two sub-domains: a rotating mesh (a circular area that incorporates the blades, with 1.2 m diameter), and a fixed mesh (outside the former). The rotating sub-domain modelled the rotation of the turbine. During a complete rotation, one can compute the resulting force [5], the torque, the power and the efficiency of the isolated turbine (tower).

The boundary conditions used for the isolated turbine were: inflow with a specified velocity (U_∞ = 1 m/s), turbulent intensity of 0.2 and turbulence length scale of 0.1 (as presented in Georgescu et al [5]) on the left hand side of the domain; zero pressure on the right hand side of the domain; slip symmetry on the upper and lower boundaries; logarithmic wall function on the blades; neutral identity pair on the boundaries between the fixed and rotating sub-domains. The resulted velocity field is plotted in Fig. 15.

After setting up the two-dimensional numerical model for a farm consisting of 7 staggered turbines on two non-overlapped rows, where each of the turbines used a rotating mesh sub-domain, the computations had to be stopped after several days, as the progress was insignificant (less than 5%). So, a quicker method had to be derived, as in Antheaume et al [10] and Georgescu et al [11; 12], to study farm configurations, namely an approach that couples a macroscopic non-rotational model of the turbine with a calculation using the $k-\varepsilon$ turbulence model in the Rotating Machinery/ Transient Analysis options of Chemical Engineering Module of COMSOL Multiphysics.

Within that innovative numerical procedure, derived to model the unsteady flow inside a hydropower farm equipped with several parallel Achard turbines (towers), in different configurations, the "main turbine" (main tower) is the only one that turns at constant angular velocity ω during the simulations. To reduce the computational effort, the idea was to replace all but one of the rotating turbines (towers), by "fictitious turbines" (fixed-ones) that would yield on the flow the same effect as the rotating turbines. Even if the fictitious turbines are non-rotating during computations, outside and especially downstream of each fictitious turbine, the flow behaviour is similar to the one of the main turbine; differences are due to the inter-influence of all turbines, the main-one and the fictitious-ones.

5.1 Force Coefficients and Average Power Coefficient for an Isolated Turbine

Firstly, the pressure values over each blade, recorded for the last complete rotation of the isolated turbine, were integrated to obtain the values of the forces acting on each blade, with respect to the flow direction (*Ox*), and the cross-flow direction (*Oy*), denoted F_x and F_y, and measured in N/m, as the model is two-dimensional. Then, the velocity field on the rotating sub-domain was integrated for each time step, and the resulting values of the integrals were divided by the area of the rotating mesh, in order to get average velocities U_m over the moving sub-domain at each time step. The force coefficients c_{F_x} and c_{F_y} on the turbine, for each time step, were obtained by normalizing the values of F_x and F_y by the term $\rho U_m^2 D/2$, where ρ is the water density

Secondly, F_x and F_y were composed to yield the values of the tangential forces F_t acting on each blade, at each time step. By adding for each time step the values of the tangential force F_t on the 3 blades, one gets the resulting total tangential force, then multiplying the result with the turbine radius (D/2), one gets the value of the thrust on the turbine shaft, as a discrete function of time (time step), for a full rotation. By averaging these discrete values of the thrust for a full rotation, we get the average trust acting on the isolated turbine (tower). Finally, by multiplying the average thrust with the angular velocity ω, we compute the power of the turbine, and normalizing the result by the power of the fluid, $\rho U_\infty^3 D/2$, we find the average power coefficient c_P of the turbine, i.e. the turbine (tower) efficiency η. The efficiency of an isolated turbine resulted equal to η = 0.269.

5.2 Force Coefficients for the Farm Model and Overall Efficiency of the Farm

We need to compute unit area averaged force coefficients, $c_{F_x m}$ and $c_{F_y m}$, on *Ox*- and *Oy*-directions for the isolated rotating turbine, and associate them to the "main turbine" of the proposed numerical procedure, in order to use them to create the "fictitious turbines".

Firstly, circular sub-domains were defined in the farm numerical model, corresponding to the turbine (tower) swept area and representing the fictitious turbines. Thus, the fictitious turbines were geometrically represented by simple non-rotational circular domains, with the same diameter ($D + d$) as the swept area of the turbine, where d is the blade thickness. Within each fictitious circle, the resulting force corresponding to the main turbine was spread as unit volume force (or unit area force for two-dimensional simulations) over the whole non-rotational circular domain. Inside the non-rotating domain of each fictitious turbine, one cannot expect to obtain flow behaviour somehow similar to the one of the main turbine; in fact, the fictitious turbines represent an average over a full rotation of the main turbine.

The force coefficients computed on *Ox*- and *Oy*-directions for the isolated turbine were averaged on a complete rotation, to obtain average force coefficients on the turbine. Then, the resulting averaged coefficients were divided by the area that represents the fictitious turbine in the farm model - the area of a circle with diameter ($D + d$). The resulting values represent unit area averaged force coefficients, denoted as $c_{F_x m}$ and $c_{F_y m}$. Further, those coefficients were considered as constants in the farm model. Finally, according to the action-reaction principle, one can add in the circular non-rotational sub-domains of the fictitious turbines (towers) the volume forces computed as:

$$F_x = -c_{F_x m}\frac{\rho}{2}\left(u^2+v^2\right) \quad \text{and} \quad F_y = -c_{F_y m}\frac{\rho}{2}\left(u^2+v^2\right) \tag{1}$$

where u and v are the two local cell velocity components on the two directions *Ox* and *Oy* respectively, i.e. resulting from each iteration of the solver, for each cell in the sub-domain.

Thus, one can get outside of the fictitious turbine area, a mean flow similar to the one produced by a rotating turbine (tower), averaged over a complete rotation.

The rotating turbine, denoted as the main-one, was the only one used to compute the power of a turbine at different positions in the farm. To do that, for each numerical model of the farm, the main turbine was placed with its axis in the point of coordinates $\{x = 0; y = 0\}$, while the fictitious turbines were placed around it, in different configurations that enabled us to compute the power of the main turbine in the key positions denoted from B_1 to B_4 in Fig. 6.

For farm configurations with 2 parallel rows of turbines (towers) put in non-overlapped staggered arrangements, the turbines of the downstream row are not placed in the wake of the upstream turbines, so the average power coefficient of each turbine, i.e. its efficiency, can be computed as for the case of an isolated turbine, as the ratio between the power of the turbine, and the power of the fluid $\rho U_\infty^3 D/2$. The overall efficiency of the farm will be the ratio between the sum of the power of all turbines, and the total power of the fluid $N\rho U_\infty^3 D/2$, where N is the number of turbines in the farm.

For farm configurations with 2 parallel rows of turbines (towers) put in overlapped staggered arrangements, meaning with distances $L_y < 2D$, one cannot obtain the efficiency of a single turbine placed on the downstream row, but one can compute the average efficiency of a turbine belonging to a pair formed by an upstream turbine and the nearest downstream turbine. That average efficiency is the ratio between the sum of the power of each turbine in the selected pair, and the power of the fluid corresponding to the pair of turbines, defined as $\rho U_\infty^3 L_y/2$ (for that case, the available kinetic energy of the water entering the pair of overlapped turbines is spread over the distance L_y).

For example, in the case of the farm configuration from Fig. 6, there are 3 such pair of turbines, namely the pair formed with turbines in B_3 and B_4 positions, the pair formed with turbines in B_2 and B_1 positions, and the pair that follows below; there is a single turbine that cannot be included in a pair, namely the one placed on the first row at the bottom of the frame in Fig. 6. So, for that configuration, the farm global efficiency can be computed as the ratio between the sum of the power of all 7 turbines, and the total power of the fluid, defined over the distance $(3L_y + D)$ as: $\rho U_\infty^3 (3L_y + D)/2$.

6. Results on the Global Efficiency of the Hydropower Farm

Several numerical models of the farm were built, in order to quantify the global efficiency of the farm. For two rows of staggered turbines (towers), the influences of the spacing L_x between adjacent rows, and of the spacing L_y between axes of adjacent turbines on each row, were investigated. The following ranges of values were considered: $L_x = 2D \div 3D$, with a step of $0.25D$ for $L_y = 2D$ kept constant; $L_y = 1.5D \div 2.25D$, with a step of $0.05D$ for $L_x = 2D$, and $L_y = 2.25D \div 3D$, with a step of $0.25D$ for $L_x = 2D$ kept constant.

To ensure the free flow conditions around the farm, the computational domain extension was the same for all tested configurations, namely: 12 turbine diameters long (from $x = -5$ m to $x = 7$ m along the flow direction), and 56 turbine diameters wide (from $y = -28$ m to $y = 28$ m across the flow).

For a farm configuration with 2 parallel rows of 7 turbines put in a non-overlapped staggered arrangement, with $L_y = 2D$, the following results were obtained: $\eta = 0.4426$ for B_1; $\eta = 0.2633$ for B_2; $\eta = 0.3246$ for B_3; and $\eta = 0.3025$ for B_4, obviously the most advantaged position being B_1. The resulting farm global efficiency is $\eta = 0.3176$.

The results can be extrapolated to more than 7 turbines in the farm. For any odd number of turbines in the farm, where $N \geq 7$, the best overall efficiency is obtained with $(N + 1)/2$ turbines on the downstream row, due to the fact that the number of turbines placed in B_1 increases, and that particular position has the greatest efficiency.

The optimum global farm efficiency was obtained for a hydropower farm configuration with two parallel rows of 7 turbines (towers) put in an overlapped staggered arrangement, with $s = 0.25D$ and $L_y = 1.75D$.

The mesh for a farm configuration, with 2 rows of 7 turbines overlapped with $s = 0.25D$ and $L_y = 1.75D$, having 4 fictitious turbines placed on the first row, and the main turbine placed on the downstream row, in B_1 position between 2 fictitious turbines, consists of an unstructured mesh with almost 59000 degrees of freedom. The corresponding velocity field is plotted in Fig. 16. The fictitious turbines were separated from the main flow domain by neutral boundaries, while the rest of the boundary conditions used were the same as in the isolated turbine numerical model. For the farm configuration from Fig. 15, the efficiency of a turbine from the pair formed by turbines in B_2 and B_1 is $\eta = 0.3837$. The resulting global efficiency of the farm reaches $\eta \cong 0.35$.

For the farm configuration with 2 rows of 7 turbines overlapped with $s = 0.25D$ and $L_y = 1.75D$, having the main turbine placed on the upstream row, in B_2 position between 2 fictitious turbines, and 4 fictitious turbines placed on the downstream row, the velocity field is plotted in Fig. 17. The global efficiency of that farm is $\eta = 0.3732$, which is the best computed value, being 1.17 times greater than the value obtained for non-overlapped rows. By extrapolation, the farm overall efficiency increases when increasing the number of turbines, e.g. $\eta \cong 0.38$ for $N = 21$ turbines.

In Section 2, it was mentioned that the total tangential force can be increased, by arranging the towers within the farm in staggered parallel rows. This was confirmed by the above numerical results.

For consistency, the polar representation of the total tangential force F_t for a turbine in B_1 position in a non-overlapped farm configuration with 2 rows of 7 turbines and $L_y = 2D$, is superposed in Fig. 15 to the F_t variation for a turbine in B_1 in the overlapped configuration from Fig. 16 where $L_y = 1.75D$, and to the F_t of the isolated turbine, all of them with respect to the time moment of the full rotation.

Obviously, the maximum value of the total tangential force, and the greatest minimum value, resulted for the non-overlapped case, yielding the greatest power of a turbine in B_1 position. But when analysing the overall efficiency of a farm, the best results corresponds to the overlapped case, because the total power of the fluid decreases.

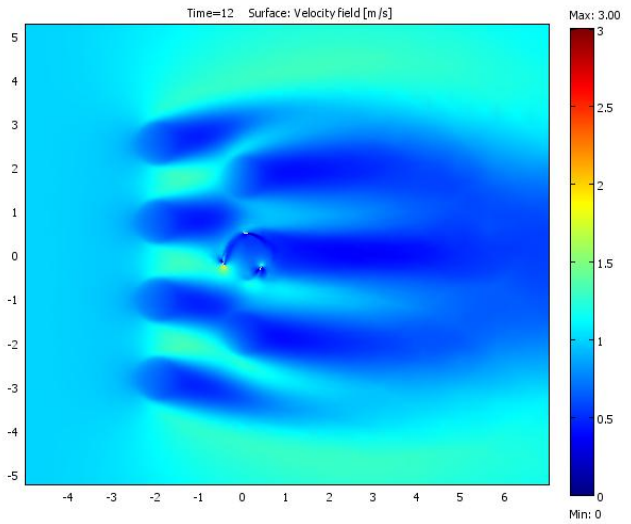

Fig. 16 Velocity field for a farm with 7 turbines on 2 parallel rows, overlapped with 0.25*D*; the main turbine is placed in B_1

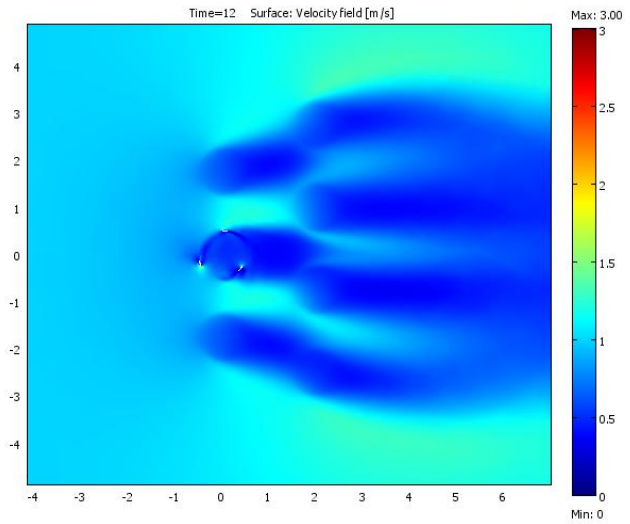

Fig. 17 Velocity field for a farm with 7 turbines on 2 parallel rows, overlapped with 0.25*D*; the main turbine is placed in B_2

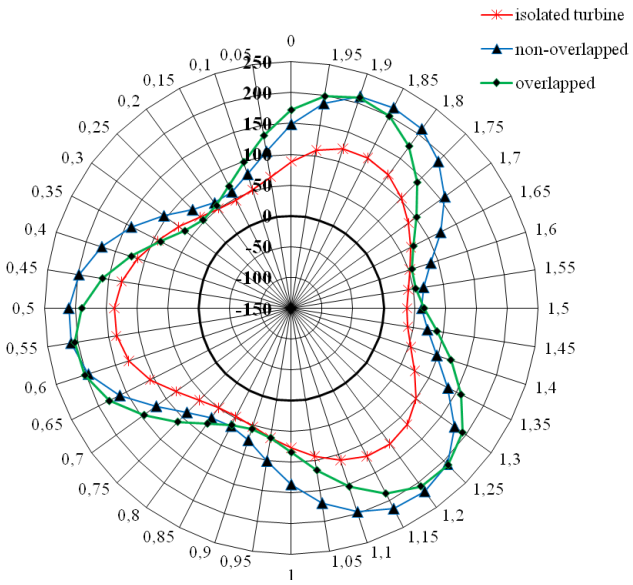

Fig. 18 Total tangential forces versus time

7. Conclusion

The study pointed on the Achard turbine, a new concept of vertical cross-flow marine turbine. Two-dimensional numerical modelling was performed in a horizontal cross-section of a hydropower farm equipped with three Achard turbines, for 3 different spatial arrangements of the turbines, using FLUENT and COMSOL Multiphysics. Numerical models validation with experimental results was performed through the velocity distribution, depicted by Acoustic Doppler Velocimetry, in the wake of the middle turbine within each farm model. Numerical velocity distribution and experimental points are somehow similar. A better fit seems to occur for the triangular farm models. The discrepancy is probably due to the fact that for the experimental models, water can by-pass the turbines, by flowing above or below, not only sideways as in the 2D numerical simulations.

In order to depict the global efficiency of the farm, the 2D modelling of the unsteady flow inside a hydropower farm, equipped with 7 Achard turbines (towers of superposed Achard turbine modules), placed on two parallel rows in staggered non-overlapped, or overlapped arrangements, has been performed using COMSOL Multiphysics. The innovative numerical procedure used here allowed determining the global efficiency of the hydropower farm, by saving a lot of computational time (each computation took about 10 hours instead of several days). The efficiency of each turbine, computed for some specific spatial position within the farm, allows depicting by extrapolation the overall efficiency of bigger farms. The overall efficiency of the farm increases when increasing the number of turbines, staggered on two rows.

Some trends with respect to the optimal arrangement of Achard turbines (towers) in a hydropower marine farm resulted. Rows of staggered overlapping parallel towers ensure the increase in global efficiency of the farm. The optimal distance between two

successive axes across the flow direction equals 1.75 turbine diameters. The quasi-optimised configuration proposed here ensures a global efficiency value greater than the best value of the global efficiency obtained for farms with non-overlapped parallel rows.

Acknowledgments

Special thanks are addressed to Dr Jean-Luc Achard, CNRS Research Director, from LEGI Grenoble, for consultancy on the Achard turbine.

Nomenclature

B	Number of blades [–]
c	Airfoil chord length [m]
c_F	Force coefficient [–]
c_P	Average power coefficient [–]
d	Blade thickness [m]
D	Turbine (runner) diameter [m]
F	Force [N]
H	Turbine (runner) height [m]
k	Turbulent kinetic energy (kinetic energy of turbulent fluctuations per unit mass) [m^2/s^2]
L_x	Space between two adjacent rows [m]
L_y	Distance between axes of 2 adjacent turbines, on each row [m]
N	Number of turbines in a farm [–]
R	Turbine (runner) radius [m]
s	Overlapping between upstream turbine and the nearest downstream turbine [m]
u	Cell velocity component on *Ox*-direction [m/s]
U_m	Average velocity in the rotating sub-domain [m/s]
U_∞	Upstream velocity of the water [m/s]
v	Cell velocity component on *Oy*-direction [m/s]
w	Relative velocity [m/s]
x	Coordinate along the main flow direction [m]
y	Coordinate across the main flow direction [m]
y^+	Dimensionless sublayer-scaled distance [–]
z	Vertical Cartesian coordinate [m]
α	Angle of attack [deg]
ε	Dissipation of turbulence per unit mass [m^2/s^3]
η	Turbine (or farm) efficiency [–]
λ	Tip speed ratio ($= \omega R / U_\infty$) [–]
ϖ	Specific turbulent dissipation rate [s^{-1}]
ω	Angular velocity [rad/s]
ωR	Transport velocity [m/s]
ρ	Water density [kg/m^3]
σ	Solidity ($= cB / R$) [–]
θ	Azimuthal angle [deg]

Subscripts

m	Averaged
n	Normal direction
t	Tangential direction
x, y	*Ox*- and *Oy*-directions

References

[1] J.-L. Achard and T. Maître, 2006, Hydraulic Turbomachine, FR Patent No. EP1718863 (A1).
[2] Georgescu, A.-M., Georgescu, S.-C., and Bernad, S. I., 2008, "Inter-Influence of the Vertical Axis, Stabilised, Achard Type Hydraulic Turbines – THARVEST," Final Report CEEX Project No. 192/2006, Bucharest, http://www.tharvest.ro
[3] Georgescu, A.-M., Georgescu, S.-C., Bernad, S. I., and Hasegan, L. V., 2008, "Staggered Arrangement of Three Bladed, Vertical Axis, Cross-Flow Turbine Towers in Farms," Scientific Bulletin "Politehnica" University of Timisoara, Trans. on Mechanics, Vol. 53, No. 67, pp. 63-68.
[4] Georgescu, A.-M., Georgescu, S.-C., and Bernad, S. I., 2008, "Innovative Simplified 2D Numerical Modelling of the Inter-Influence of Vertical Axis Cross-Flow Turbines Mounted in Hydropower Farms," Sci. Bull. "Politehnica" University of Timisoara, Trans. on Mechanics, Vol. 53, No. 67, pp. 57-62.
[5] Georgescu, A.-M., Georgescu, S.-C., Degeratu, M., Bernad, S., and Cosoiu, C. I., 2007, "Numerical Modelling Comparison Between Airflow and Water Flow within the Achard-Type Turbine," 2nd IAHR WG on Cavitation and Dynamic Problems in Hydraulic Machinery and Systems, Timisoara, Romania, pp. 289-298.
[6] Georgescu, A.-M., Georgescu, S. C., Cosoiu, C. I., Alboiu, N., and Hamzu, Al., 2010, "Velocity Field in the Wake of a Hydropower Farm Equipped with Achard Turbines," IOP Conf. Ser.: Earth Environ. Sci., Vol. 12, 012108, pp. 1-10.
[7] Wilcox, D. C., 1994, Turbulence Modeling for CFD, 2nd edition, DCW Industries Inc., La Cañada, California.
[8] Blazek, J., 2001, Computational Fluid Dynamics: Principles and Applications, Elsevier, Oxford.
[9] Georgescu, A.-M., Georgescu, S.-C., Cosoiu, C. I., Alboiu, N., and Petre, A.-M., 2010, "Experimental Versus Numerical Results on the Velocity Field in the Wake of a Hydropower Farm Equipped with Three Achard Turbines," University "Politehnica" of Bucharest Scientific Bulletin, Series D, Vol. 72, No. 1, pp. 133-140.
[10] Antheaume, S., Maître, T., and Achard, J.-L., 2007, "An Innovative Modelling Approach to Investigate the Efficiency of Cross Flow Water Turbine Farms," Sci. Bull. "Politehnica" University of Timisoara, Trans. Mech., Vol. 52, No. 66, pp. 281-288.
[11] Georgescu, A.-M., Georgescu, S.-C., and Bernad, S. I., 2008, "A Method to Assess the Inter-Influence between vertical Axis, Cross-Flow Turbines in a Free Stream – 2D Numerical Modelling," COMSOL Conference 2008, Budapest, Hungary, pp. 45-51.
[12] Georgescu, S.-C., Georgescu, A.-M., Bernad, S. I., and Susan-Resiga, R., 2009, "Overall Efficiency of Hydropower Farms Consisting of Multiple Vertical Axis, Cross-Flow, Marine Current Turbine Modules," CMFF'09, Budapest, Vol. 2, pp. 752-759.